Available online at www.sciencedirect.com
SCIENCE DIRECT®
International Journal of Heat and Mass Transfer 48 (2005) 1898–1908
International Journal of HEAT and MASS TRANSFER
www.elsevier.com/locate/ijhmt

Convective heat and solute transfer in partially porous cavities

D. Gobin *, B. Goyeau, A. Neculae [1]

FAST-UMR 7608 (CNRS, Universities Paris VI and Paris XI) Campus Universitaire, Bât. 502, 91405 Orsay Cedex, France

Received 26 April 2004; received in revised form 21 December 2004
Available online 4 March 2005

Abstract

This paper deals with natural convection driven by combined thermal and solutal buoyancy forces in a binary fluid. The configuration under study is a confined enclosure partially filled with a vertical porous layer. The mathematical description of the problem is based on a one-domain formulation of the conservation equations. The set of numerical results presented here quantitatively shows the influence of the porous layer on the flow structure and on heat and species transfer in the enclosure.

The paper is focused on the analysis of the influence of the characteristic parameters governing double diffusive convection, namely the ratios of solutal and thermal parameters: the diffusivities and the buoyancy forces. Heat and mass transfer is analyzed as a function of the permeability of the porous layer. It is shown that the coupling of the flow penetration in the porous layer with the combined buoyancy forces induces a specific behavior of the flow structure and average heat transfer in the enclosure.

Keywords: Double diffusion; Thermosolutal convection; Porous medium; Fluid–porous interface

1. Introduction

Heat and solute transport by convection in fluid or porous domains is relevant to a wide range of industrial processes or environmental situations. Among these the analysis of heat or mass transfer due to natural convection has been the subject of a very intense research activity over the past decades, and documented reviews are available to the interested reader [1,2].

The present paper deals with a particular subclass of such problems where natural convection takes place in a confined enclosure partially filled with a porous medium. Heat transfer and fluid flow through fibrous insulation [3], natural convection heat and mass transfer in solidification [4], or solute exchange in sediments in coastal environments [5] are some examples of the fields where transport phenomena take place at an interface between a fluid phase and a porous medium. The context of the present study aims at a better understanding of convective heat and solute transfer in the mushy zone of a solidifying multi-component system, where natural convection is known to be driven by combined thermal and solutal buoyancy forces in a binary fluid. This particular class of convection is termed thermosolutal or double diffusive convection. In the following paper we refer to a very simple model in the absence of phase change where the dendritic region is represented as an homogeneous porous medium.

* Corresponding author.
E-mail address: gobin@fast.u-psud.fr (D. Gobin).
[1] Present address: Faculty of Physics, West University of Timisoara, 300223 Timisoara, Romania.

0017-9310/$ - see front matter © 2005 Elsevier Ltd. All rights reserved.
doi:10.1016/j.ijheatmasstransfer.2004.12.016

Nomenclature

A	aspect ratio, H/L
C	solute mass fraction, wt%
$\mathscr{D}$	mass diffusivity of the solute, m^2/s
Da	Darcy number, K/H^2
g	acceleration of gravity, m/s^2
H	height of the enclosure, m
$\vec{k}$	unit vector (vertical direction)
k	thermal conductivity, W/(m·K)
K	permeability (m^2)
L	width of the enclosure, m
Le	Lewis number: α/D
N	buoyancy ratio: $\beta_C \Delta C/\beta_T \Delta T$
Nu	average Nusselt number: $\int_0^1 -(\partial\theta/\partial x)\mathrm{d}z$
P	dimensionless pressure
Pr	Prandtl number, ν/α
Ra_S	solutal Rayleigh number, $N\,Le\,Ra_T$
Ra_T	thermal Rayleigh number, $g\beta_T \Delta T\, H^3/\alpha\nu$
Sh	average Sherwood number: $\int_0^1 -(\partial\phi/\partial x)\mathrm{d}z$
T	dimensional temperature, K
$\vec{V}$	dimensionless fluid velocity ($\vec{v^*}H/\alpha$)
w (u)	vertical (horizontal) component of $\vec{V}$
x_P^*	dimensional width of the porous layer, m
x_P	dimensionless width of the porous layer, (x_P^*/L)
$x(z)$	dimensionless coordinates, $x^*/H(z^*/H)$

Greek symbols

α	thermal diffusivity, m^2/s
β_T	thermal expansion coefficient: $-1/\rho_0(\partial\rho/\partial T)$
β_C	solutal expansion coefficient: $-1/\rho_0(\partial\rho/\partial C)$
ΔC	concentration difference
ΔT	temperature difference
ε	porosity of the porous layer
μ	dynamic viscosity of the fluid, kg·m/s
ν	kinematic viscosity, m^2/s
ϕ	dimensionless concentration, $\phi = (C - C_0)/\Delta C$
ψ	stream function: $u = -\partial\psi/\partial z$; $w = \partial\psi/\partial x$
ρ	fluid density
θ	dimensionless temperature, $\theta = (T - T_0)/\Delta T$

Subscripts

eff	effective property of the porous layer
F	refers to the fluid domain
P	refers to the porous medium
S or C	solutal parameter
T	thermal parameter

A complete overview of double diffusive convection in fluid or porous layers is not within the scope of the present introduction, and we will only briefly recall the main studies on convection in composite cavities where the fluid domain is partially occupied by a porous layer.

It should first be noticed that very few experimental papers are available on the topic [6–8], and that the main effort has been to address the numerical simulation of such flows. The mathematical description of the conservation laws at a fluid–porous interface has been the topic of many studies after the first approach presented by Beavers and Joseph [6], and the problem of using one- or two-domain formulations for the conservation equations has been extensively discussed in the literature (see [9]).

The problem of *thermal* convection for such a configuration in a vertical enclosure where the porous layer is parallel to the vertical walls has been previously studied in the context of wall insulation [10,11,3] or solidification [12,4,13]. An exact solution has been proposed by [14] and the stability problem has been tackled by [15]. Numerical results for a vertical enclosure with two porous layers have been presented by Merrikh and Mohamad [16]. In all these studies the one-domain formulation has been used.

Another class of studies considers superimposed horizontal layers, generally a fluid on top of a porous layer. Here the main interest is to compare the stability results with the well-known critical Rayleigh numbers for Rayleigh–Bénard convection in fluid or porous layers [17,7,18]. This analysis has been then extended to the double diffusive problem, using first a two-domain formulation [19,20] and more recently a one-domain approach [21].

The present paper focuses on the simulation of double diffusive convective flows in a binary fluid, confined in a vertical enclosure, divided into two vertical layers, one porous and the other fluid. The first analysis in this field has been proposed by Gobin et al. [22], where the influence of the Darcy number of the porous layer on heat and mass transfer has been analyzed, especially in the range of very small permeabilities for different Rayleigh numbers. The study was focused on the case of aqueous solutions ($Pr = 10$; $Le = 100$) as a binary fluid.

Following this first approach, several studies have concerned a similar situation with two porous layers, one along each vertical wall, a configuration supposed to refer to thermal insulation inside buildings [23,24]. In these studies, the fluid under consideration is a mixture of air with another gaseous component($Pr \sim 0.7$) and thus the Lewis number has the usual order of magnitude for gases: $Le \sim \mathcal{O}(1)$. Considering this range of parameters ($Le < 10$) considerably limits the relevance

of the analysis since, as will be shown hereafter, the characteristics of the flow are barely different from the purely thermal case. Indeed it has been extensively shown in the literature that thermosolutal convective flows in fully fluid or porous cavities may exhibit multi-cellular flow structures and complex heat and solute transfer interaction characteristics due to the large difference between heat and species diffusivities, that is, high Lewis numbers.

The scope of the present study is to extend the parametric approach previously initiated by Gobin et al. [22] and to analyze the influence of the main double diffusive parameters, namely the Lewis number and the relative strength of the thermal and solutal buoyancy forces. The paper first present the mathematical model and the resolution technique in Section 2, then the characteristics of the porous layer are studied in Section 3 through a reference case and the influence of the geometry of the system. Finally the influence of the double diffusive parameters is presented in the last section.

2. Problem formulation

The geometry under consideration is the two-dimensional rectangular cavity (height H, total width L) sketched in Fig. 1, where the porous layer (thickness x_P^*) along the left wall is assumed to be homogeneous and isotropic. The porous medium is saturated by the binary fluid which fills the remaining of the enclosure. Different uniform temperatures and concentrations are specified at the external vertical walls of the cavity, and zero heat and species fluxes are assumed at the horizontal boundaries. The flow is assumed to be laminar and incompressible, and the binary fluid to be Newtonian and to satisfy the linear Boussinesq approximation

$$\rho = \rho_0[1 - \beta_T(T - T_0) - \beta_C(C - C_0)] \tag{1}$$

Moreover the porous matrix is supposed to be in thermal equilibrium with the fluid, and the Soret and Dufour effects are neglected.

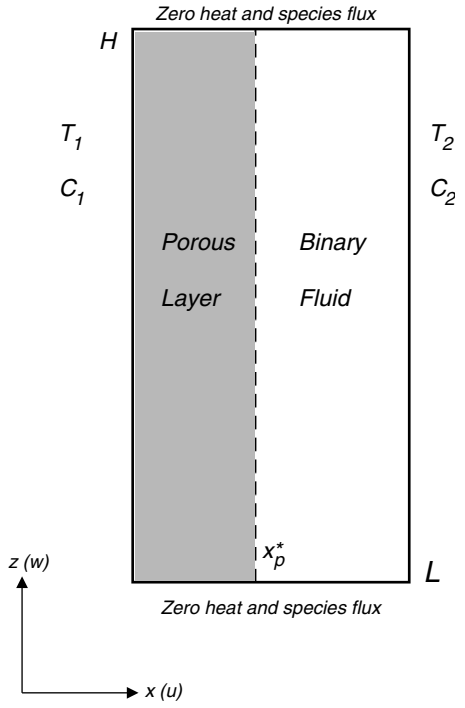

Fig. 1. Schematic description of the problem.

The mathematical model results from the coupled system of conservation equations in the fluid and in the porous region, with the appropriate boundary conditions at the fluid/porous interface. Concerning momentum conservation, the problem of continuity between a fluid and a porous medium has been intensively studied over the last thirty years and a discussion of the different models may be found in Goyeau et al. [9]. In the present paper, we choose a one-domain approach, which considers the porous layer as a pseudo-fluid and the composite region as a continuum. This leads to solve only one momentum equation, a modified version of the Navier–Stokes equation which includes a Darcy term, and eventually a Forchheimer term. The adequate expression of the momentum equation, for the fluid or for the porous medium, is retained through the corresponding value of the permeability [10]. This formulation has been widely used in previous numerical computations, inclusively by the present authors, since it does not require any explicit boundary condition at the fluid/porous interface. The validity of this approach has been assessed by Goyeau et al. [9] for the Poiseuille flow in a partially porous channel, in the configuration studied by Beavers and Joseph [6]. A systematical comparison with a two-domain approach has not been attempted by the authors, but the comparison presented by Zhao and Chen [21] in the context of a stability analysis shows that both formulations lead to similar results.

Under the foregoing hypotheses, the macroscopic conservation equations both retain the Darcy–Brinkman formulation in the porous layer and the Navier–Stokes equation in the binary fluid, the expression of the permeability being a prescribed function of space. In terms of the dimensionless variables defined in the nomenclature, the steady-state macroscopic conservation equations resulting from the present model are written

$$\vec{\nabla}.\vec{V} = 0 \tag{2}$$

$$\frac{1}{\varepsilon^2 Pr}(\vec{V}\cdot\vec{\nabla})\vec{V} = -\frac{\vec{\nabla}P}{Pr} + Ra_T(\theta + N\phi)\vec{k} - \frac{1}{Da}\vec{V} + \frac{\mu_{\text{eff}}}{\mu}\nabla^2\vec{V} \tag{3}$$

$$\vec{V}\cdot\vec{\nabla}\theta = \frac{k_{\mathrm{eff}}}{k}\nabla^2\theta \tag{4}$$

$$\vec{V}\cdot\vec{\nabla}\phi = \frac{1}{Le}\frac{\mathscr{D}_{\mathrm{eff}}}{\mathscr{D}}\nabla^2\phi \tag{5}$$

At the boundaries, zero heat or species flux conditions are prescribed at the horizontal walls and Dirichlet boundary conditions at the vertical walls: $\theta = \phi = -0.5$ at the porous medium external wall (x = 0) and $\theta = \phi = 0.5$ at the vertical wall in contact with the fluid ($x = 1/A$).

The problem is characterized by the set of dimensionless parameters generally defined for double diffusive convection in fluids, plus the parameters characterizing porous media:

1. The thermal Rayleigh number defined with the *fluid* properties, Ra_{T},
2. The buoyancy ratio N,
3. The Prandtl and Lewis numbers of the fluid, Pr and Le,
4. The Darcy number (dimensionless permeability) of the porous layer, Da,
5. Geometrical parameters, the aspect ratio of the enclosure A, and the reduced thickness of the porous layer, x_P.

μ, k and $\mathscr{D}$ refer to the *fluid* viscosity, thermal conductivity and molecular diffusivity, respectively, while subscript 'eff' refers to the corresponding *effective* property of the porous medium. The Nusselt and Sherwood numbers are the dimensionless average heat and mass fluxes along the vertical walls. All definitions are given in the nomenclature.

The set of Eqs. (2)–(5) is numerically solved using a standard finite volume procedure. The detailed description of the method may be found elsewhere and only specific features of the method are recalled hereafter. The method has been successfully used by the authors to solve heat and fluid flow problems in fluids and porous media in similar ranges of parameters. It has been first verified that thermal and thermosolutal natural convection results for $x_{\mathrm{P}} \to 1$ at any value of the Da number were in agreement with the standard Darcy–Brinkman version of the code [25]. It has also been assessed that, at high values of the Darcy number (1 and more), the results at any value of x_{P} were identical to the results obtained for the pure fluid problem [26]. The calculations for thermal convection in fluid/porous cavities have been successfully compared against the existing results [3].

Depending on the permeability of the fluid layer, the strong temperature, concentration or velocity gradients may be located along the vertical walls or in the vicinity of the fluid–porous interface. Consequently, for low and intermediate permeabilities, compound meshes are necessary in order to solve the interfacial zone and limit the computational cost: two distinct irregular (generally sinusoidal) horizontal grids are taken in the porous layer and in the fluid cavity. The number of nodes in each domain depends on the Rayleigh numbers and on the relative thickness of the porous region. For higher Darcy numbers (typically $Da > 10^{-3}$) a single sinusoidal distribution of nodes may be used in the horizontal direction. Typical numbers of nodes for the horizontal direction range between 145 and 252. In the vertical direction the spatial distribution is generally regular, usually from 202 up to 402 nodes for describing multi-cellular structures.

3. Role of the porous layer characteristics

Our purpose is to characterize the main features of double diffusive convection in a partially porous enclosure. The configuration under study leads to seven governing parameters if one excludes the ratios of the effective properties and it is not within reach to explore combinations of all the dimensionless numbers. We thus restrict our analysis to a selected range of parameters which we believe is relevant to understand the underlying mechanisms. First we will mainly refer here to the case of aqueous solutions which have been often used in the experimental approach of double diffusion, and also as an archetypal binary system for solidification experiments. As a consequence the Prandtl number of the binary fluid is fixed ($Pr = 10$) and the corresponding Lewis number is imposed at a value of 10^2, except when the influence of the Lewis number on the flow characteristics is studied. Also the aspect ratio of the cavity is fixed ($A = H/L = 2$). Moreover only the case of cooperating thermosolutal convection is considered (the thermal and solutal body forces are acting in the same direction). It is well-known that double diffusive flows in vertical fluid enclosures with Dirichlet temperature and composition conditions at the active walls may give rise to multi-cellular "thermosolutal" structures under given conditions [27], namely a high Lewis number, a sufficiently high thermal Rayleigh number (boundary layer regime) and a dominating solutal buoyancy force with a "moderate" buoyancy ratio N. Thus the typical reference situation is defined as: $Pr = 10$, $A = 2$, $Le = 100$, $Ra_{\mathrm{T}} = 10^6$ and $N = 10$.

In a first stage of this study [22], we had focused our attention on the influence of the permeability of the porous layer at different thermal Rayleigh numbers, for given Prandtl and Lewis numbers, the geometry of the layer/enclosure system and the buoyancy ratio being kept fixed. The numerical results had shown that the heat transfer dependance on the Darcy number is characterized by a non-intuitive behavior where the Nusselt number undergoes a minimum with increasing permeability. The strong modification of the flow struc-

ture when the flow penetrates the porous medium is attributed to the thermosolutal feature of the process. The scope of the present analysis is to focus more closely on this aspect, and we aim at characterizing the role of the buoyancy ratio and of the Lewis number on a wide range of variation for the permeability of the porous layer through the Darcy number.

It might be worth of interest to analyze the role of the *effective* transport properties appearing in the coefficients of the diffusion terms in (3)–(5). This would be justified if we were willing to account for the detailed description of a specific porous structure, including the porous matrix tortuosity and dispersion phenomena or permeability anisotropy, or even evolving heterogeneities. At this stage of our work, this is not within the scope of the present report. This is why the ratios of the effective transport coefficients to the fluid properties are taken equal to 1 in the scalar conservation equations and the effective viscosity in the Brinkman term is also taken equal to the fluid viscosity $\mu_{\text{eff}} = \mu$.

The results are mainly presented in terms of the average dimensionless mass (or heat) flux at vertical walls, the Sherwood (or Nusselt) number. Let us underline that, due to the reference length which is used to define the dimensionless variables, the mass flux (respectively, the heat flux) is defined with respect to $\mathscr{D}\Delta C/H$ (respectively, $k\Delta T/H$), so that the Sherwood number (respectively, Nusselt number) for pure diffusion (pure conduction) is $H/L = A$ (here, 2 in all our calculations).

Two limiting cases may be considered: the limit $Da \to \infty$ (in practice, $Da = 1$) which corresponds to a fully fluid cavity, and the limit $x_P = 1$, corresponding to a completely porous cavity, with different permeabilities, according to the Darcy number. In both cases, the results have been carefully checked, and the Sherwood number correlations previously assessed for fluid [27] or porous [25] domains are recovered.

3.1. Influence of the layer thickness

It has been previously assessed [22] that the thickness of the porous layer has a significant influence on heat and mass transfer in the enclosure, even for small values of x_P. This can be seen here from the results displayed in Fig. 2 showing the variation of the Sherwood number for a given permeability of the porous domain ($Da = 10^{-5}$).

This influence is seen to be limited in this case to $x_P < 0.1$, since for thicker porous layers (between 0.20 and 0.9) the Sherwood number is not very sensitive to x_P. For $x_P \to 1$, however, a slight decrease of Sh may be noted on the curve. This effect has also been observed on the Nu results proposed by [11]. It shows that the mass (heat) transfer is enhanced in the presence of an even very thin fluid layer along the wall. This is one of the interpretations of the Brinkman no slip effect at the wall [28].

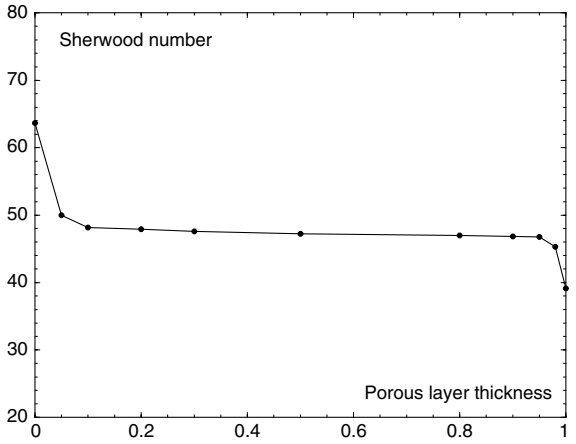

Fig. 2. Average mass transfer variation as a function of the porous layer thickness at $Da = 10^{-5}$ ($Ra_T = 10^6$, $N = 10$, $Le = 100$, $Pr = 10$, $A = 2$).

If we display the variation of the average mass transfer as a function of the Darcy number for different values of the porous layer thickness, several observations may be done (Fig. 3a). It may be first observed that when the permeability of the porous layer increases from very low values ($Da \sim 10^{-9}$) to high values corresponding to a fluid ($Da \sim 1$), the Sherwood number is continuously increasing. A second feature is that, compared to the pure fluid cavity ($x_P = 0$, here represented by the result at $Da = 1$), the influence of the porous layer thickness on the mass transfer decrease is essentially visible in the low permeability range ($Da < 10^{-7}$). In this range the comments made on Fig. 2 apply for different values of the Darcy number. At higher permeabilities, the presence of the porous layer induces a drastic decrease of the Sherwood number even for a small thickness ($x_P = 0.1$) of the porous layer, but there is almost no sensitivity to x_P.

If we now consider the evolution of the average heat transfer with the same variations of Da and x_P (Fig. 3b), the first observation is that this evolution is no longer monotonous. This feature will be examined in the forthcoming section. The second observation is the strong sensitivity of the heat transfer characteristics to the porous layer thickness at all permeabilities in the [0.1–0.8] range. Simulations performed for thick porous layers ($x_P \geqslant 0.8$, not shown) indicate that the average Nusselt number remains very close to the pure conduction limit ($Nu = A = 2$) over a wide range of Darcy numbers, emphasizing the absence of convective heat transfer in this range. This shows that the effect of the porous layer thickness on the boundary layers is not the same for species distribution and for the thermal field: we will show

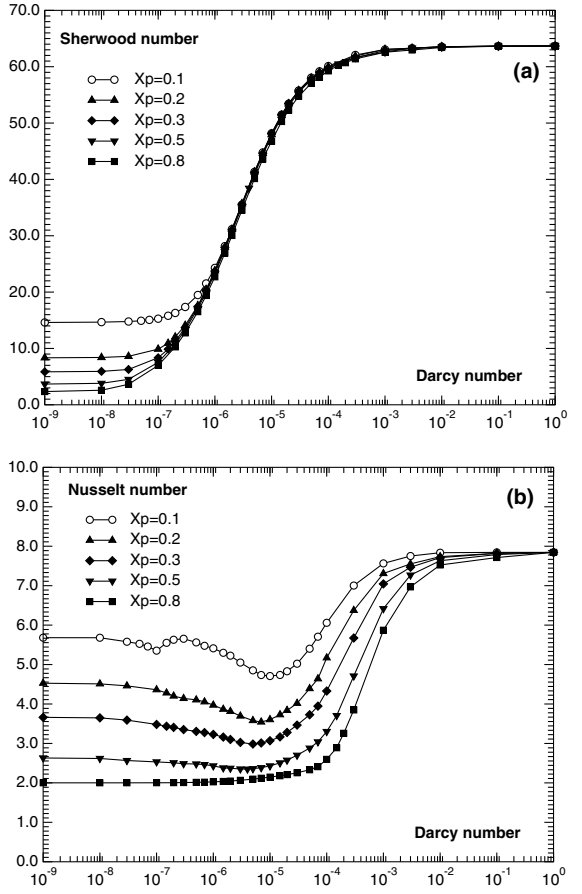

Fig. 3. Mass (a) and heat (b) transfer variation with permeability for different porous layer thicknesses ($Ra_T = 10^6$; $N = 10$; $Pr = 10$; $A = 2$; $Le = 100$).

that this is due to the difference in diffusion lengths for θ and ϕ and thus to the Lewis number.

3.2. Reference case

In this section the analysis of the results is presented for the standard reference configuration defined above ($Ra_T = 10^6$, $N = 10$, $Pr = 10$, $Le = 100$, $A = 2$) and $x_P = 0.1$. The results displayed in Fig. 3a at $x_P = 0.1$ show the Sherwood number variation with the permeability of the porous layer (the Darcy number). As commented above the overall evolution is easily explained and confirms the observations made for heat transfer in similar situations in the case of pure thermal convection. In the low permeability range ($Da < 10^{-7}$), the porous layer behaves like a solid wall, where the diffusive decrease of temperature and concentration in the layer results in a significantly less active convection compared with the fluid case ($x_P = 0$). Then with increasing permeability, the flow penetrates the porous domain and the

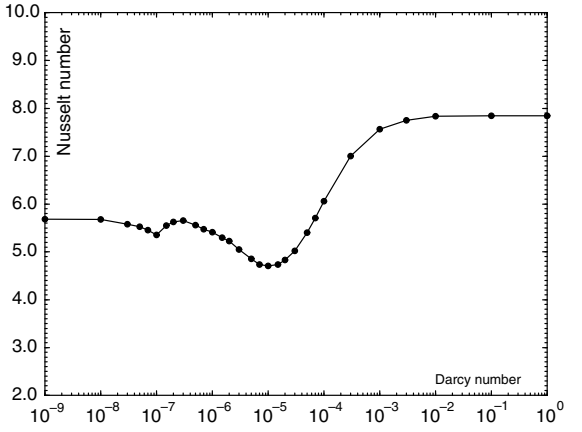

Fig. 4. Heat transfer variation with permeability for the reference case: $Ra_T = 10^6$; $N = 10$; $Pr = 10$; $Le = 100$; $A = 2$; $x_P = 0.1$. (This curve is displayed in white circles in Fig. 3b, Fig. 9b, Fig. 11b.)

corresponding mass transfer monotonously increases, and finally for very high permeabilities ($Da > 10^{-3}$), the friction in the porous layer becomes negligible and the Sherwood number gets to a constant value, corresponding to the solution obtained for a fully fluid cavity.

If we turn our attention to the variation of the average heat transfer with permeability for $x_P = 0.1$ (Fig. 4), we observe that the variation of Nu is essentially different. The Nusselt number does not increase monotonously with increasing permeability, but it exhibits two minima. Although less apparent, these minima still exist at lower values of Ra_T (not shown). This new feature, compared to the results presented by Gobin et al. [22] where only the main minimum had been identified, will help us to refine the analysis of the phenomenon. The evolution of the convective flow with increasing permeability results from the competition between two opposing effects. First, the higher permeability results in a better penetration of the porous layer by the flow and consequently in a smaller diffusive damping of the imposed temperature and concentration difference in the layer. The effective temperature and composition gradients governing the buoyancy forces are then expected to grow and the flow to be accelerated, resulting in higher heat and mass transfer. This is what may be observed on the Sherwood number. On the other hand, due to the difference between the diffusivities, the central recirculation loop driven on the scale of the thermal boundary layer thickness is driven by a relatively smaller temperature difference. Locally the thermal buoyancy force decreases, and the intensity of the internal thermal loop is decreasing, and so does the average heat transfer. The double diffusive process is thus dominating the evolution and the foregoing analysis is intended to refine the interpretation of this behavior in terms of the

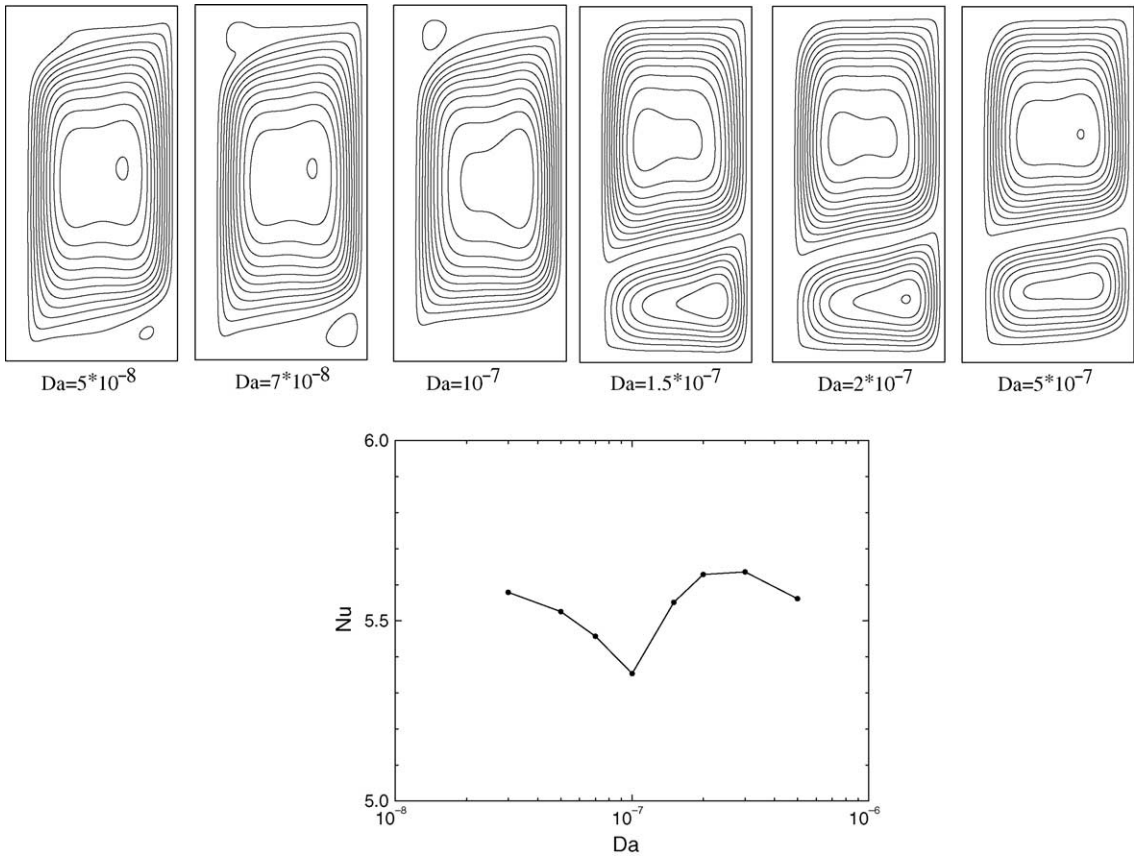

Fig. 5. Reference case—heat transfer and flow structure around the first minimum: $5\times10^{-8} < Da < 5\times10^{-7}$; $\Delta\psi = 0.1$ ($Ra_T = 10^6$, $N = 10$, $x_P = 0.1$, $Le = 100$, $Pr = 10$, $A = 2$). For comparing the flow structures, the streamlines have been plotted using the maximum value of the ψ_{max} for all cases ($\psi = 0$ at the walls and $\Delta\psi = 0.1$).

thermosolutal features of the solution. First, when displaying the streamlines at different values of the Darcy number, it is clearly seen (Figs. 5 and 6) that the existence of a minimum is directly related to the flow structure. In the neighborhood of the first minimum (Fig. 5), one may observe that the decrease in the Nusselt number is caused by a decrease of the main recirculation cell, due to the formation of a low velocity zone in the bottom part of the enclosure where the heat transfer is mainly conductive. This "stagnant" zone is compositionally stratified (see Fig. 7) as in typical double diffusive problems [26], while the heat transfer in this region is mainly conductive. With the increasing height of the stagnant zone, the local vertical concentration gradient decreases and gets destabilized by the lateral temperature gradient, resulting in the formation of a secondary co-rotative cell and a sudden increase of the Nusselt number (Fig. 5). Then the formation process of a stagnant zone at the bottom of the enclosure resumes at $Da \sim 2\times10^{-7}$ with the related decrease in heat transfer, until the development of a third recirculation cell allows for a new enhancement of the average heat transfer (Fig. 6). Then, the increase in Darcy number results in the penetration of the porous layer by the flow, until, at very high permeabilities a fully centro-symmetrical multi-cellular structure characteristic of double diffusion in liquids is recovered.

The evolution of the process is well illustrated in Fig. 8 where the maximum of the stream function in each cell is displayed. One can see that the decrease of the flow in the initial recirculation cell is continuous up to Da on the order of 3×10^{-5}. The corresponding decrease of the heat transfer is stopped by the formation of a second cell due to the destabilization of the stagnant zone. The sharp minimum observed in the Nusselt number curve is due to the fact that immediately after its sudden formation the second cell is very active, with a value of ψ_{max} almost as high as the first cell. Then the intensity of this new cell decreases as a new stagnant zone is formed at the bottom. The third cell on the contrary appears very progressively and the heat transfer increase at these Darcy numbers seems to be related to the progressive penetration of the porous layer by the flow. The increase occurs around $Da = 10^{-5}$ far beyond the destabilization

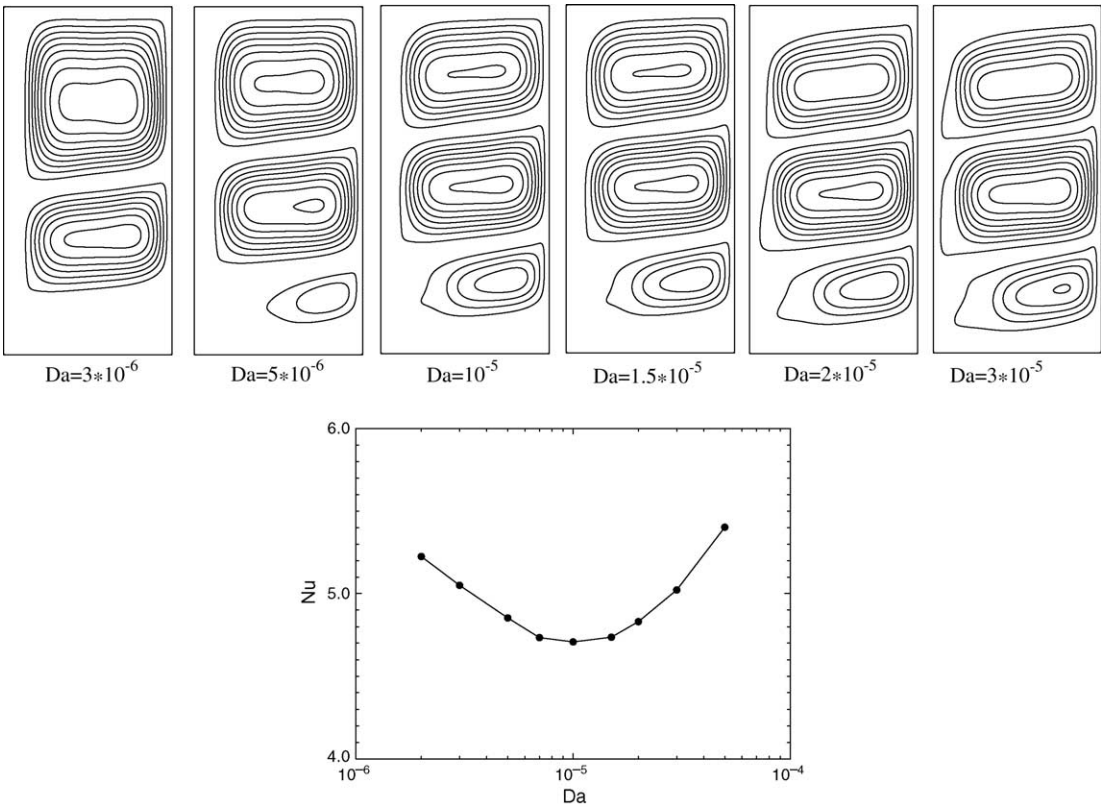

Fig. 6. Reference case—heat transfer and flow structure around the main minimum: $3\times10^{-6} < Da < 3\times10^{-5}$; $\Delta\psi = 0.1$ ($Ra_T = 10^6$, $N = 10$, $x_P = 0.1$, $Le = 100$, $Pr = 10$, $A = 2$).

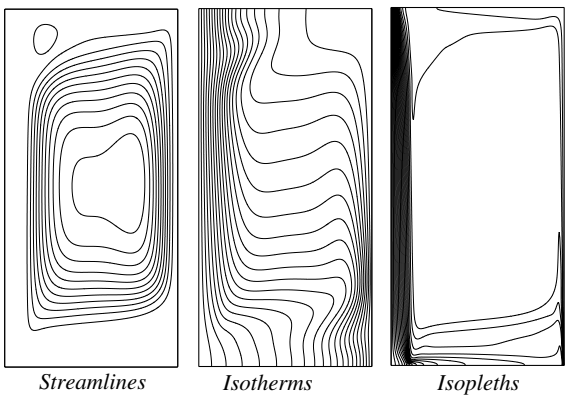

Fig. 7. Flow, temperature and composition fields at $Da = 10^{-7}$ ($Ra_T = 10^6$, $N = 10, x_P = 0.1$, $Le = 100$, $Pr = 10$, $A = 2$).

of the stagnant zone which occurs at $Da = 3\times10^{-6}$ (Figs. 6 and 8). The third cell then continuously increases in size and intensity to reach the level of the first cell at high Da values ($\sim10^{-2}$) when the cavity is practically fluid and the flow structure is symmetrical with respect to the center of the cavity.

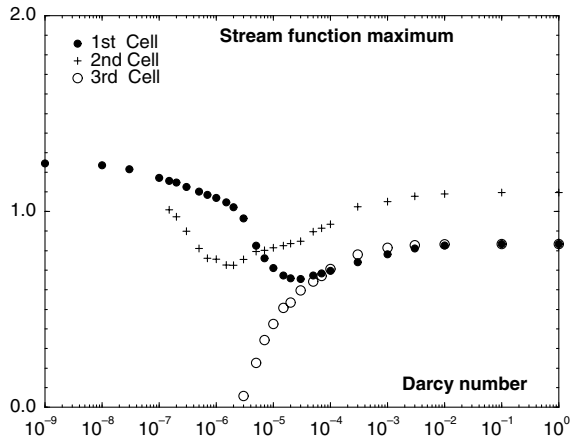

Fig. 8. Reference case—stream function maximum as function of permeability ($Ra_T = 10^6$, $N = 10$, $x_P = 0.1$, $Le = 100$, $Pr = 10$, $A = 2$).

4. Influence of double diffusive parameters

The previous analysis has shown that the leading mechanism in the variations in heat transfer clearly

has a double diffusive origin. The purpose of the forthcoming section is to support this analysis with complementary simulation results where the influence of the main parameters of thermosolutal convection is investigated, namely the Lewis number *Le* and the buoyancy ratio *N*.

4.1. Influence of the Lewis number

As already mentioned the specific features of double diffusive convection appear when the characteristic diffusion lengths for heat and solute are significantly different. The parameter which governs the ratio between thermal and molecular diffusivity (the Lewis number) is generally on the order of 10^2 or more for liquids. Note that for gases $Le \sim 1$ and for such low Lewis numbers, the scale of heat and solute boundary layers are similar and the buoyancy forces have a merely additive effect. No multi-cellular structure is expected and the dependence of the Nusselt number with permeability follows the same variation as the Sherwood number, a smoothly monotonous increase, as displayed in Fig. 9. Even if the low and moderate values of the Lewis numbers used in the simulations are not realistic, the comparison is intended to show its influence on the heat and mass transfer characteristics. All the parameters are fixed, except for the mass diffusivity, meaning that the solutal Rayleigh number is increased in the same proportion as the Lewis number. The Sherwood number is uniformly increased with *Le*, and it can be verified that in the "fluid limit" ($Da = 1$) the classical correlation [27] is verified. Clearly the Nusselt number variation is similar at low values of the Lewis number ($Le \leqslant 5$), and the heat transfer is decreasing as *Le* increases, as expected from the scaling laws in the solutally dominated regime ($N > 1$) [29]. The Nusselt curve shows only one minimum for $Le = 10$. As can be seen in Fig. 10, the flow structure remains *monocellular* but one can see a difference between an outer recirculation cell, driven by the solutal effect and a decreasing inner thermal cell (not shown) which almost vanishes in the region of the minimum ($Da \sim 10^{-5}$), where the decrease in heat transfer is compensated around $Da = 3 \times 10^{-5}$ by the penetration of the porous layer. The mechanism is thus similar to the second minimum of the reference case described above.

4.2. Influence of the buoyancy ratio

The last feature to be analyzed is the influence of the buoyancy ratio. It is also well known that the double diffusive feature of the flow is mostly visible in the intermediate regime between the heat transfer dominated ($N \ll 1$) and the mass transfer dominated ($N \gg 1$) regimes. In this range, both buoyancy forces are in competition, and their relative influence may be analyzed. In this section numerical results are presented for positive

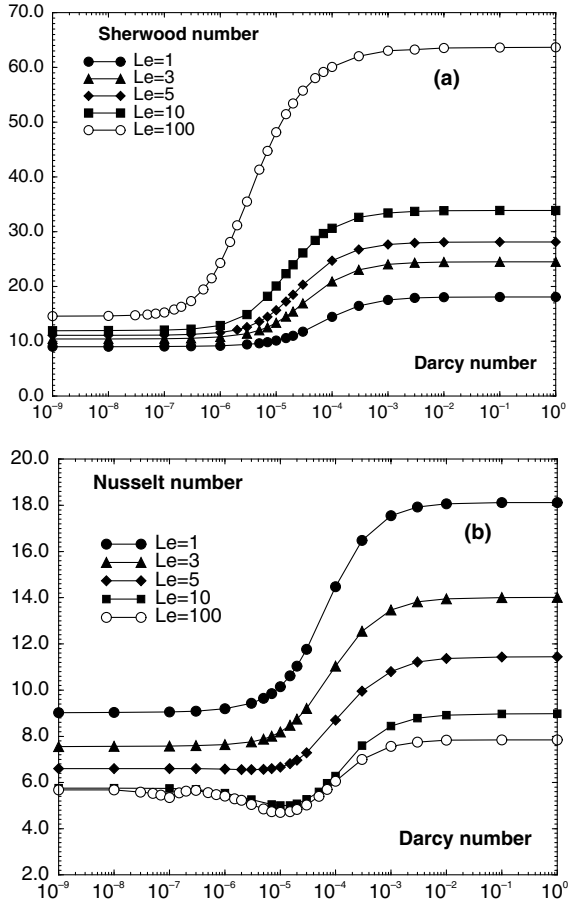

Fig. 9. Mass (a) and heat (b) transfer variation with permeability for different Lewis numbers ($Ra_T = 10^6$; $N = 10$; $Pr = 10$; $= 2$; $x_P = 0.1$).

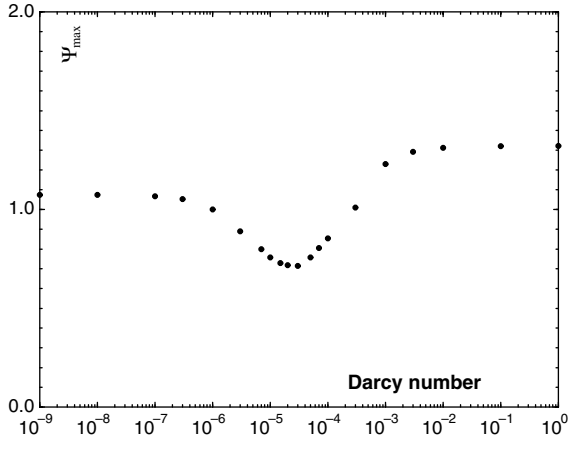

Fig. 10. Stream function maximum as function of permeability ($Ra_T = 10^6$, $N = 10$, $x_P = 0.1$, $Le = 10$, $Pr = 10$, $A = 2$).

values of N ranging from 1 to 10 for the same set of parameters, including $Le = 100$ (Fig. 11). The results may be compared to the reference case for decreasing values of the solutal Rayleigh numbers, that is, when decreasing the imposed composition difference between the vertical walls.

Concerning the Sherwood number (Fig. 11a), it may be observed that the value of N has very little influence at low Da values: only the increase in mass transfer occurs at smaller Da for higher N. Then, in the "fluid" range ($Da > 10^{-3}$), the dependence of Sh on N is in agreement with the scaling laws (see [27]).

If we consider the Nu curves (Fig. 11b), there is almost no difference between $\beta_C \Delta C/\beta_T \Delta T = 1$ or 2, for which the Nusselt number variation is monotonous. A minimum may be noticed at $N = 3$, but the limiting values (at $Da < 10^{-7}$ or $Da > 10^{-3}$) are also identical: here only the solutal Rayleigh number is modified through N and it is known to have little influence on the Nusselt number. At $N = 3$, one could show that the flow structure remains *monocellular*, a stagnant zone is formed at the bottom of the enclosure in the intermediate range of permeabilities, which results in a decrease of the average heat transfer. In this particular situation this zone remains stable, because the flow penetration of the porous layer accelerates the fluid before the stratified zone gets destabilized.

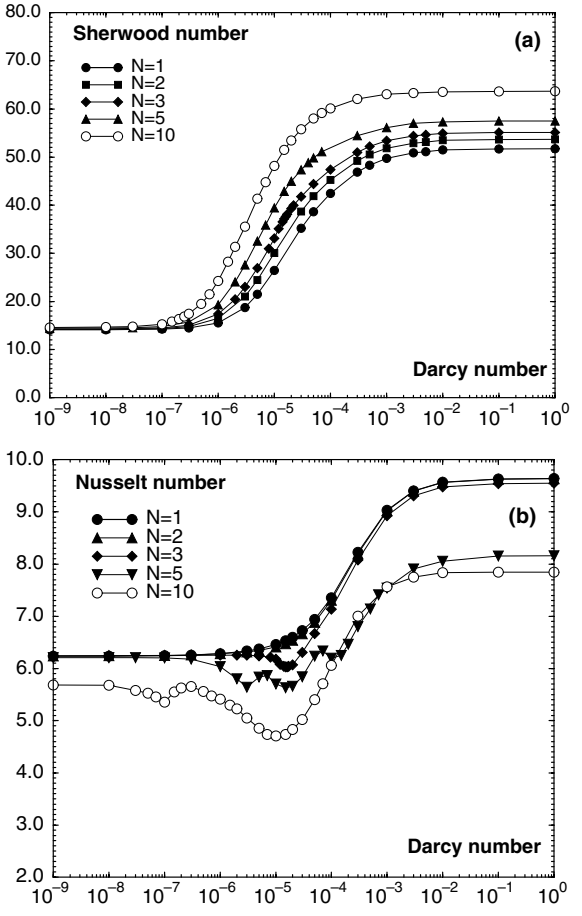

Fig. 11. Mass (a) and heat (b) transfer variation with permeability for different buoyancy ratios ($Ra_T = 10^6$; $Pr = 10$; $Le = 100$; $A = 2$; $x_P = 0.1$).

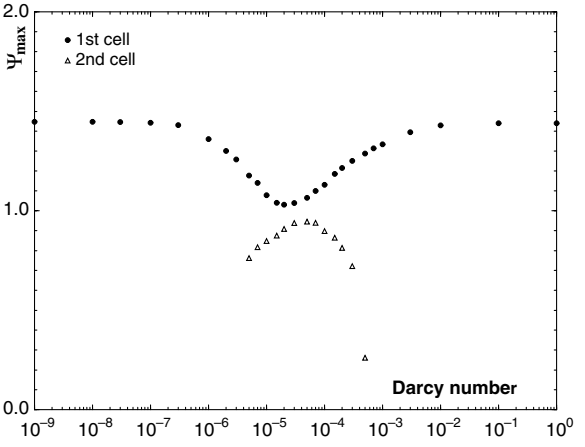

Fig. 12. Stream function maximum as function of permeability ($Ra_T = 10^6$, $N = 5$, $x_P = 0.1$, $Le = 100$, $Pr = 10$, $A = 2$).

For $N = 5$, the flow structure exhibits three minima:

- the first minimum corresponds to the formation of a second cell,
- in the neighborhood of $Da = 10^{-5}$ a stagnant zone is formed below the second cell but this zone does not reach destabilization and the second cell increases again,
- around $Da = 10^{-4}$ the flow penetration progressively increases the strength of the first cell and the second cell finally disappears,
- at high permeabilities the flow is monocellular.

This complex behavior is seen to result from a subtle shift between the minimum of the intensity of cell 1 and the maximum of cell 2 (Fig. 12). The $N = 5$ case appears as a transition between the globally monocellular flow structure obtained at $N \leqslant 3$ and the 3-cell structure at $N = 10$. At low Da, the Nusselt number value at $N = 5$ is similar to the value obtained at smaller N (Fig. 11b), while at high permeabilities the effect of solutally dominated convection may be observed in the significant decrease in heat transfer, and the Nu value gets closer to the value at $N = 10$.

5. Conclusion

The analysis of the numerical results presented in this paper clearly shows the dependence of the average heat

transfer on the double diffusive parameters. If it is confirmed that the presence of the porous layer has a strong influence on the transfers, the modification of the flow structure and the consequent modifications of the heat transfer clearly result from a competition between the flow penetration in the porous layer, depending essentially on its permeability, and the effect of the parameters related to the thermosolutal characteristics: high Lewis number and dominating solutal buoyancy force. These two ingredients are generally present in the solidification process of binary alloys and the influence of this mechanism on the solidification process should be analyzed in more detail.

Acknowledgement

The calculations have been performed on the vectorial processor of the NEC-SX5 computer of IDRIS (CNRS-Orsay) with the support of the Engineering Division of CNRS (SPI) under grant # 0336.

References

[1] A. Bejan, Convection Heat Transfer, second ed., Wiley, New York, 1995.
[2] K. Vafai, Handbook of Porous Media, Marcel Dekker Inc., New York, 2000.
[3] P. LeBreton, J.P. Caltagirone, E. Arquis, Natural convection in a square cavity with thin porous layers on its vertical walls, ASME J. Heat Transfer 113 (1991) 892–898.
[4] C. Beckermann, R. Viskanta, S. Ramadhyani, Natural convection in vertical enclosures containing simultaneously fluid and porous layers, J. Fluid Mech. 186 (1988) 257–284.
[5] I. Webster, S. Norquay, F. Ross, R. Wooding, Solute exchange by convection within estuarine sediments, Estuarine, Coast. Shelf Sci. 42 (1996) 171–183.
[6] G.S. Beavers, D.D. Joseph, Boundary conditions at a naturally permeable wall, J. Fluid Mech. 30 (1) (1967) 197–207.
[7] F. Chen, C.F. Chen, Experimental investigation of convective stability in a superposed fluid and porous layer when heated from below, J. Fluid Mech. 207 (1989) 311–321.
[8] M.F. Tachie, D.F. James, I.G. Currie, Velocity measurements of a shear flow penetrating a porous medium, J. Fluid Mech. 493 (2003) 319–343.
[9] B. Goyeau, D. Lhuillier, D. Gobin, M. Velarde, Momentum transport at a fluid–porous interface, Int. J. Heat Mass Transfer 46 (2003) 4071–4081.
[10] E. Arquis, J.-P. Caltagirone, Sur les conditions hydrodynamiques au voisinage d'une interface milieu fluide–milieu poreux: application a la convection naturelle, C.R. Acad. Sci. Paris 299 (1) (1984) 1–4.
[11] S.B. Sathe, W.Q. Lin, T.W. Tong, Natural convection in enclosures containing an insulation with a permeable fluid–porous interface, Int. J. Heat Fluid Flow 9 (4) (1988) 389–395.
[12] C. Beckermann, S. Ramadhyani, R. Viskanta, Natural convection flow and heat transfer between a fluid layer and a porous layer inside a rectangular enclosure, J. Heat Transfer 109 (1987) 363–370.
[13] M. Song, R. Viskanta, Natural convection flow and heat transfer within a rectangular enclosure containing a vertical porous layer, Int. J. Heat Mass Transfer 37 (16) (1994) 2425–2438.
[14] C. Weisman, P. Le Quéré, M. Firdaouss, Sur la solution exacte de la convection naturelle en cavité partiellement remplie d'un milieu poreux, C.R. Acad. Sci. 327 (1999) 235–240.
[15] J. Mercier, C. Weisman, M. Firdaous, P. Le Quéré, Heat transfer associated to natural convection flow in a partly porous cavity, ASME J. Heat Transfer 124 (2002) 130–143.
[16] A.A. Merrikh, A.A. Mohamad, Non-Darcy effects in buoyancy driven flows in an enclosure filled with vertically layered porous media, Int. J. Heat Mass Transfer 45 (2002) 4305–4313.
[17] D.A. Nield, Onset of convection in a fluid layer overlying a layer of a porous medium, J. Fluid Mech. 81 (1977) 513–522.
[18] F. Chen, C.F. Chen, Convection in superposed fluid and porous layers, J. Fluid Mech. 234 (1992) 97–119.
[19] F. Chen, C.F. Chen, Onset of finger convection in a horizontal porous layer underlying a fluid layer, J. Heat Transfer 110 (1988) 403–409.
[20] J.-J. Valencia-Lopez, J.A. Ochoa-Tapia, A study of buoyancy-driven flow in a confined fluid overlying a porous layer, Int. J. Heat Mass Transfer 44 (24) (2001) 4723–4736.
[21] P. Zhao, C.F. Chen, Stability analysis of double-diffusive convection in superposed fluid and porous layers using a one-equation model, Int. J. Heat Mass Transfer 44 (2001) 4625–4633.
[22] D. Gobin, D. Goyeau, J. Songbe, Double diffusive natural convection in a composite fluid–porous layer, ASME J. Heat Transfer 120 (1998) 234–242.
[23] M. Mharzi, M. Daguenet, S. Daoudi, Thermosolutal natural convection in a vertically layered fluid–porous medium heated from the side, Energy Conv. Manag. 41 (2000) 1065–1090.
[24] R. Bennacer, H. Beji, A.A. Mohamad, Double diffusive convection in a vertical enclosure inserted with two saturated porous layers confining a fluid layer, Int. J. Therm. Sci. 42 (2) (2003) 141–151.
[25] B. Goyeau, J. Songbe, D. Gobin, Numerical study of double-diffusive natural convection in a porous cavity using the Darcy–Brinkman formulation, Int. J. Heat Mass Transfer 39 (7) (1996) 1363–1378.
[26] D. Gobin, R. Bennacer, Cooperating thermosolutal convection in enclosures: 2. Heat transfer and flow structure, Int. J. Heat Mass Transfer 39 (13) (1996) 2683–2697.
[27] R. Bennacer, D. Gobin, Cooperating thermosolutal convection in enclosures: 1. Scale analysis and mass transfer, Int. J. Heat Mass Transfer 39 (13) (1996) 2671–2681.
[28] S. Turki, G. Lauriat, An examination of two numerical procedures for natural convection in composites enclosures, in: Proceedings of AIAA–ASME Thermophysics and Heat Transfer Conference, HTD. Vol. 130, 1990, pp. 107–113.
[29] A. Bejan, Mass and heat transfer by natural convection in a vertical cavity, Int. J. Heat Fluid Flow 6 (3) (1985) 149–159.